RESEARCH ARTICLE

CrossMark

Aster Mapping of Limestone Deposits and Associated Lithounits of Parts of Chikkanayakanahalli, Southern Part of Chitradurga Schist Belt, Dharwar Craton, India

H. T. Basavarajappa[1] · L. Jeevan[1] · S. Rajendran[2] · M. C. Manjunatha[1]

Abstract

Economically viable limestone deposits are mostly formed by calcite minerals, and these minerals are widely used in manufacturing of cement, mortar, fertilizer and flux for smelting of iron ores, and mapping of such deposits is significant and important in scientific research. This study examines the capability of Advanced Spaceborne Thermal Emission and Reflection Radiometer (ASTER) with the wavelength range visible–near-infrared and short-wave infrared spectral bands to map such limestone carbonate deposits and associated lithounits occurred in and around of Chikkanayakanahalli, southern part of the Chitradurga schist belt using minimum noise fraction (MNF) and decorrelation stretching methods. The study results that (1) the RGB image of MNF (R: B1; G: B2; B: B3) of ASTER is capable of discriminating the limestones and associated different rock types, namely banded magnetite quartzites (BMQ), graywackes, Mn- and Fe-rich cherts, meta-basalts, granitic gneisses, granitoids and migmatites and (2) the decorrelation stretch image of ASTER bands 8, 3, 1 of the ASTER delineated clearly the limestones and associated rocks of the study area. Study of spectral signatures of field samples of such economic limestones in the wavelength of 350–2500 nm using Fieldspec3 Spectroradiometer showed the spectral absorption near 2.32 μm due to the presence of calcite minerals in the rocks. The results of study are cross-verified in the study area and confirmed through petrological and chemical analyses of the samples. This study bespeaks the potential of ASTER sensor and application of image processing methods to map the economic limestone deposits and associated rocks of the study area.

Keywords ASTER · Chikkanayakanahalli · MNF · Decorrelation · Limestone · Spectroradiometer

Introduction

Most of the economic limestone deposits are calcite bearing rocks widely used in civil construction materials and in iron ore smelting (Hamilton et al. 1995). Remotely sensed satellite images are capable of showing them and allow scientists to map them economically in short time before detailed mapping and exploration of such deposits. Studies were carried out to discriminate the carbonate formations using spectral signatures of the rock bearing mineral, namely calcite, to target the spatially occurred economic deposits studying their diagnostic absorption signatures (Rajendran and Nasir 2014a, b; Gaffey 1986a, b, 1987; Crowley 1986). Also, several research studies showed that it is important to compare the satellite image spectra of the target with field/laboratory spectra of samples of the area to analyze and study the reliability of diagnostic absorption features of the end members. For mapping the surface exposures of limestones that occurred in variable sizes in the tropical region, researchers use different image processing mapping methods. In the exploration of minerals and ore deposits, the spectral bands of ASTER have been

✉ H. T. Basavarajappa
basavarajappaht@gmail.com

L. Jeevan
jeevannarayan8885@gmail.com

S. Rajendran
sankaranrajendran@yahoo.com

[1] Department of Studies in Earth Science, CAS in Precambrian Geology, University of Mysore, Mysore, Karnataka, India

[2] Department of Earth Sciences, College of Science, Sultan Qaboos University, Muscat, Oman

🌐 Springer

used well for delineating such deposits and associated lithology (Ali et al. 2009; Bedini 2011; Brandmeier 2010; Crosta et al. 2003; Haselwimmer et al. 2011; Zhang et al. 2007). ASTER indices are used for delineating carbonate minerals (Rajendran et al. 2011; Mars and Rowan 2010; Kalinowski and Oliver 2004; Rowan and Mars 2003; Sanjeevi 2008). The data have also been used successfully for delineating limestones (Crowley 1986; Rajendran and Nasir 2014a, b). This study uses ASTER spectral bands and image processing methods to map the limestone deposits and associated lithounits that occurred in and around of Chikkanayakanahalli, southern part of the Chitradurga schist belt (CSB), India (Fig. 1), situated in the tropical region since limited studies were conducted under tropical weathering setup. Here, the limestones are characterized using ASTER image by studying the spectral feature logged in the ASTER bandwidth, and an attempt is done to analyze the diagnostic spectral features of limestone deposits of the study area in the laboratory.
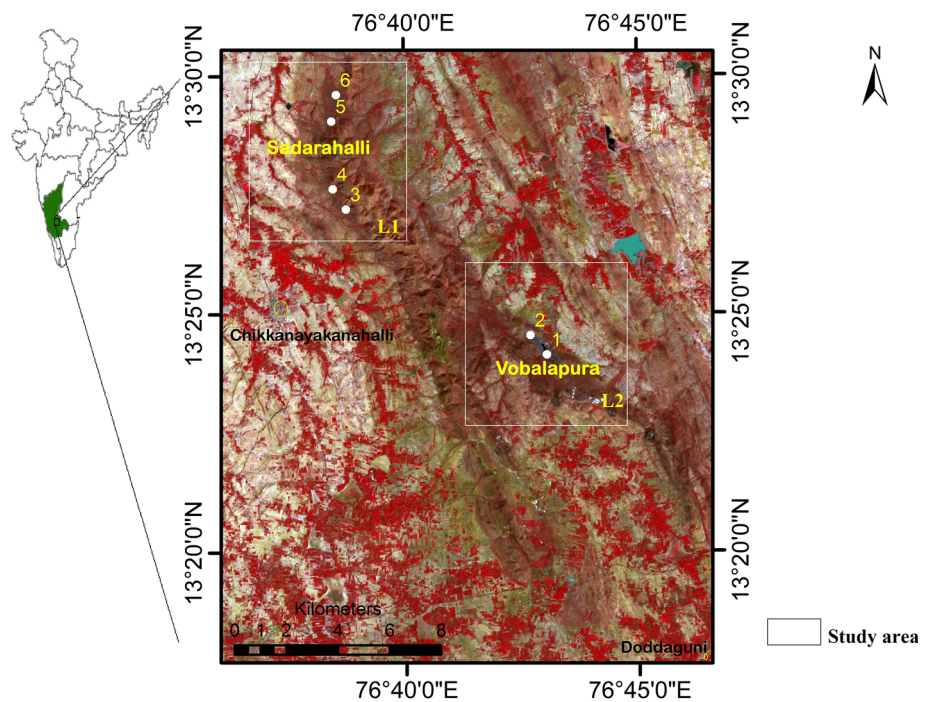
Geological Settings

The 25 km of length and 15 km of width Chikkanayakanahalli schist belt is located in the southern extension of Chitradurga schist belt. The general physiographic trend of the Chikkanayakanahalli schist belt is North–South, whereas the occurrence of schistose rocks trend NNW–NW and exhibit dips ranging from 30° to 80° (average 55°). Radhakrishna (1952) subdivided the rocks

of the area into an upper 'Doddaguni series' and a lower 'metamorphic series.' Srinivasan and Srinivas (1972) proposed a geosynclinal scheme of evolution for the rocks of the Dharwar group and described the rocks of the Doddaguni series, which forms part of the Dharwar Supergroup, as geosynclinal shelf sediments belonging to the second cycle of sedimentation in the evolutionary cycle of the Dharwar. Mukhopadhyay et al. (1981) and Mukhopadhyay and Ghosh (1983) carried out detailed structural mapping around Doddaguni area and concluded that the rocks in the area have been affected by multiple episodes of deformation.

The study area in and around of Chikkanayakanahalli is located between the North latitude of 13°18′00″ to 13°30′00″ and East longitude of 17°34′00″ to 76°45′00″, and it covers approximately an area of 525 sq. km (Fig. 1). The rock formations in the area are subdivided into two main groups, viz. (1) the older group made up of amphibolite and chlorite schist interbedded with quartzite and (2) the younger group consisting of BIF, marble, pelitic and semi-pelitic schists with amphibolite (Table 1; Fig. 2; Swaminath et al. 1976). Here, the lateritoid manganese deposits are associated with discontinuous exposures of oligomictic conglomerate and demarcate the boundary between the two groups. The older group has been correlated with Bababudan Group and the younger group with the Chitradurga group by Mukhopadhyay et al. (1981, 2006), Ramakrishna and Vaidyanadhan (2008). The supracrustal rocks are folded into antiforms and synforms and later subjected to metamorphism in green schist to


Fig. 1 ASTER (RGB: 3, 2, 1) image shows the study area (L1 (Sadarahalli range) and L2 (Vobalapura range))

Table 1 Lithostratigraphic succession and classification of Chikkanayakanahalli schist belt (Modified after Anantha Murthy 1980)

Geological processes	Precursor lithologies present lithologies
Mainly chemical sediment	
Basic igneous intrusion	Dolerites
Ferruginous sediments	Iron formations
Manganiferous sediments	Meta phyllite
Carbonate sediments	Carbonates
Detrital sediments	Chlorite schist
Aluminous sediments	Quartzite and some meta-arkose paragneiss
Siliceous sediments	
Gradational unconformity	
Granitic intrusion/early Precambrian granite crust	Gneisses

Fig. 2 Geology of the study area (after Geological Survey of India, 1993)
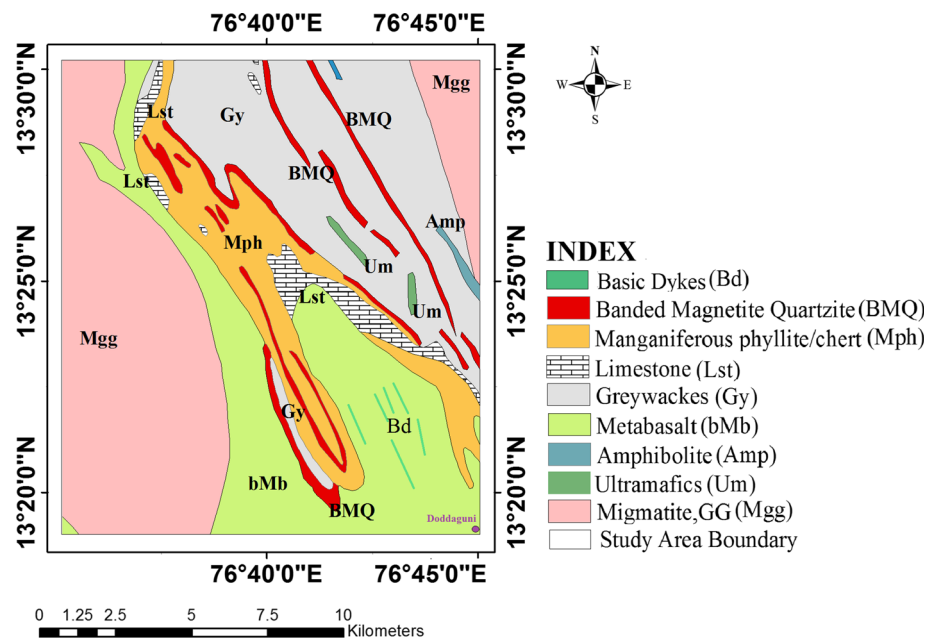
amphibolite facies. The geology of the study area is provided in Fig. 2.

Here, quartzite, chlorite schist, carbonate and dolerite are the younger lithounits overlaid on the older rocks of peninsular gneiss. The quartzite and carbonate are at places associated with iron and manganese formations. Here, the occurrence of carbonate rocks is essentially made up of cherty dolomite and limestone, the former predominating over the latter. These carbonate rocks are associated with occurrence of manganese which has been noted in the phyllites (Garrels 1960). Dolomite and limestone occur as beds (reef like) with limited outcrop width, starting from Doddaguni and continuing along the western margin of Chitradurga schist belt. Devaraju and Anathmurthy (1977, 1984) opined that precipitation of limestone marked the beginning of carbonate deposition in an open basin with low salinity, pH and Mg/Ca ratio. This event was followed by deposition of dolomite and ankerite under lagoonal conditions with restricted circulation of water under high salinity conditions, high pH, temperature and Mg/Ca ratios. Srinivasan et al. (1989) reported that the stromatolitic limestone of Doddaguni is in the proximity of manganese mineralization occurred in the southeastern part of Chikkanayakanahalli area. Table 1 shows the lithostratigraphic succession of the study area.

Satellite Data and Methods

ASTER satellite sensor was launched on December 18, 1999 at Vandenberg Air Force Base, California, USA, orbiting to the sun-synchronous path with an inclination 98.3° degree from the equator. The repeating ground track coverage of a place repeats for every 16 days. The ASTER

sensor consists of three separate instrument subsystems and 14 bands information with varying spatial resolution: (1) VNIR: 1–3 bands—15 m resolution (2) SWIR: 4–9 bands—30 m resolution (3) TIR: 10–14 bands—90 m resolution (Yamaguchi et al. 1999; Abrams 2000; Ali et al. 2009; Rajendran and Nasir 2014a, b, c). In this study, the nine ASTER spectral bands of VNIR–SWIR regions obtained at Japan Space System/ERSDAC (ASTL1A 0401140535200401241074) dated on January 14, 2004 are used after preprocessing to map the limestones (ENVI 2009; Green et al. 1988; Ghosh and Chatterjee 1990; Guha et al. 2012a, b) and associated rocks of the study area by simple image processing methods, namely minimum noise fraction (MNF) and decorrelation stretching image processing methods.

ENVI version 4.8 software package is used to process the datasets like ASTER, and Fast Line-of-sight Atmospheric Analysis of spectral bands/Spectral Hypercubes (FLAASH) is the known atmospheric correction algorithm involved in the preprocessing of data using ENVI (Pour and Hashim 2011a, b; Pournamdari et al. 2014a, b). The innate dimensionality of ASTER is revealed by transformation of principal component analysis, decorrelation stretch method and minimum noise fraction transformation. Spectral bands of 8, 3 and 1 are used in decorrelation stretch method for studying the spectral characters of limestones. MNF and PCA transformations are commonly done to compress and sort the multivalued pixels and to enhance multispectral remote sensing data. Signal-to-noise ratio should be maximum, and accordingly, it holds more information, and this is mainly done through linear transformation specifically designed by MNF transformation (Rajendran and Nasir 2014a, b).

The minimum noise fraction is almost similar to principal component analysis, and in other way, we can say it as a double-time PCA because it reduces the data and increases the signal-to-noise ratio. Here, MNF is applied to ASTER bands VNIR–SWIR spectral bands to map limestones and associated rock types of the study area.

The final output images of this method are described and cross-checked in the field using available geology map in the scale of 1:50,000. Further, samples were collected during the field work (Table 2) and used to collect spectra in the wavelength of 350–2500 nm using Fieldspec3© Spectroradiometer in the laboratory. Spectroradiometer has finer spectral resolution (3 nm in 700 nm and 10 nm from 1400 to 2100 nm) and good signal-to-noise ratio with finer spectral sampling interval (from 350–1050 nm, it is 1.4 nm and from 1000–2500 nm, it is 2 nm) (ASD Inc. 2012). The spectral resolution is good enough to detect the related absorption spectral characteristic of the constituent minerals of the limestones. Field samples were collected over the field outcrop of limestones in two different locations: the Sadarahalli range (L1) and Vobalapura range (L2) (Fig. 1). Details of the rock sample locations are given in Table 2 and Fig. 1. In each outcrop, two–four samples are collected for spectroscopic studies. Rock samples are cut into $4'' \times 5''$ to $5'' \times 7''$ rectangular pieces. The sample size range used is well within the size norms of the samples analyzed at the Jet Propulsion Laboratory (JPL) associated with National Aeronautics and Space Administration, USA (Baldridge et al. 2009). Ten spot observations per sample are recorded to six samples and averaged to get the characteristic spectral curve for each limestone sample. Further, spectral profiles of two or three spots are measured for each limestone sample to record the 'representative' spectra based on averaging of the spectral profiles of each spot. Averaging of multiple measurements has an added advantage in suppressing insignificant kinks in the spectral profiles of the rock.

ASTER Sensitivity and Spectral Characteristics of Carbonate Rocks

Electromagnetic radiation interacted with each and every mineral presented in the earth surface and shows a diagnostic spectral signature (Gupta 2003; Clark 1999) which holds the unique information related to the particular mineral based on their chemical and physical properties. The studies of mapping with the aid of spectral properties are carried out earlier by many researchers (Rajendran and Nasir 2014a, b; Rajendran et al. 2011; Gaffey 1985). ASTER sensor is characterized by particular spectral wavelengths near visible to infrared rays, and in this way, the diagnostic carbonate $(CO_3)_2$ absorption near the wavelengths 2.31–2.33 μm in the spectral band 8 and the

Table 2 Locations of limestone samples

Locations (in Fig. 1)	Sample no.	Geo-location	Rock type
1	CH-SN8	**N**13°24′4.544″ **E**76°43′4.387″	Limestone
2	CH-SN8A	**N**13°24′33.975″ **E**76°42′43.698″	Limestone
3	CH-SN9	**N**13°27′11.653″ **E**76°38′42.124″	Limestone
4	CH-SN9A	**N**13°27′38.766″ **E**76°39′38.472″	Limestone
5	CH-SN10	**N**13°29′0.688″ **E**76°38′29.831″	Limestone
6	CH-SN11	**N**13°29′34.047″ **E**76°38′32.065″	Limestone

ferric (Fe^{3+}) and ferrous (Fe^{2+}) irons absorptions are around 0.45 μm wavelength likely in ASTER band 1 and 1.0–1.1 μm wavelengths likely in ASTER band 3, respectively, which are helpful to discriminate iron-rich weathered surface (Rajendran and Nasir 2014a, b; Hubbard and Crowley 2005). In this way, the ASTER sensor is leading superior over other sensors for discrimination and mapping of different carbonate rocks. FCC (false-color composite) and other image processing methods are used to map these mineral deposits based on the spectral absorption characteristics (Harding et al. 1989), decorrelation stretching (Rajendran and Nasir 2014b; Philip et al. 2003) and minimum noise fraction (Rajendran et al. 2011, 2012; Rajendran and Nasir 2013; Khan et al. 2007).

The world-known deposits of carbonates rocks are extensive with the mineral assemblages of calcite and dolomite compared to other minerals like siderite, magnesite, aragonite, ankerite and rhodochrosite (Van der Meer 1995; Clark 1999; Gaffey 1985, 1986a, b, 1987). The earlier study on spectral signatures near SWIR band of ASTER for carbonate minerals is already proved by many earlier researchers with the known absorption region (Van der Meer 1994; Gaffey 1986a, b, 1987; Hunt and Salisbury 1970). All these researchers' work shows a significant difference in the precise position of calcite and dolomite mineral absorptions (Hunt and Salisbury 1970), found the calcite absorption centered at 2.35 μm and dolomite at 2.33 μm.

Spectral Absorption Characters of the Carbonate Rock of the Study Area

The limestones of Chikkanayakanahalli schist belt are detected with carbonate mineral occurrences showing deep absorption (CH SN8, SN9, SN10 and CH SN11) in wavelength range between 2300 and 2350. The laboratory spectra measured over the samples are provided in Fig. 3, which shows that all the six samples have strong absorptions around 2330 nm due to the presence of the calcite in the rocks (Boardman et al. 1995; Clark et al. 1995; Guha et al. 2012a, b; Jensen 2005). The presence of Calcite mineral is also identified through petrographic studies.

Mapping of Limestones and Associated Rocks

Decorrelation Stretching Method

Decorrelation stretch method is used in remote sensing to enhance multispectral images, and this technique is done by applying a Karhunen–Loeve transform to the colors of the image (Boardman et al. 1995; Clark et al. 1995). Occurrence and formations of limestone deposits are mapped by image

processing method, and many researchers like Gillespie and Rajendran have done extensive work by studying the spectral sensitivities of carbonate mineral formations using ASTER spectral band 8 (2.295–2.365 nm), band 3 (0.78–0.86 nm) and band 1(0.52–0.60 nm) for the study area. Among these, the eighth band responds to the presence of carbonate and hydroxyl bearing minerals of the limestone and associated formations, the third band serves to characterize the general albedo of the materials to highlight certain silicate minerals bearing rocks associated with the limestone formation, and the band 1 contains information relating to the presence of iron minerals bearing rocks associated with the limestone formations. The ASTER image of decorrelated bands 8, 3 and 1 of the study area is given in Fig. 4. It shows that almost all limestone formations occurred all along the manganiferous phyllite formation of the parts of Chikkanayakanahalli schist belt. The rock exposures are mapped and are correlated to the available geological maps (Fig. 2). Carbonate occurrences of Guddada Vobalapura (location 2) are well delineated compared to Sadarahalli deposits (location 1) located in the NW part of the study area. The spatial distribution and occurrence of formations are distinguished by brownish red color in the decorrelated RGB image (Fig. 4). The decorrelated RGB image discriminated well the occurrence of limestone (reddish brown in color) of locations 1 (L1) and 2 (L2) with the associated manganiferous phyllite occurrences. The other rocks, namely migmatitic granitic gneiss, graywacke, basic metabasalt and BMQ, discriminated well in colors of white, gray, brownish gray with green vegetation cover and orange, respectively.

Minimum Noise Fraction Method (MNF)

MNF transformation was performed on the VNIR–SWIR bands, and MNF Eigen images 4, 5 and 6 with values near to 1 are mostly noise. Thus, we excluded the MNF bands 4, 5 and 6 (Chen 2000). We used the remaining Eigen images for generating RGB image. Figure 5 shows the output of MNF bands 1, 2 and 3. In Chikkanayakanahalli schist belt (Fig. 5), the limestones are appeared in greenish yellow color. Almost all of the rock units are very well discriminated including the migmatized granitic gneiss in blue, manganiferous phyllite in orange brown, banded magnetite quartzites in orange and graywackes in gray. The contacts of litho unit are well recognizable and can be compared with the geological map (Fig. 2) of study area.

Field and Laboratory Studies

Field Characters of Carbonate Rocks

In filed, the limestone deposits occur mixed with manganese near Doddaguni area. Large deposits of limestone

Lab Spectral Data of Carbonate rocks of Chikkanayakanahalli
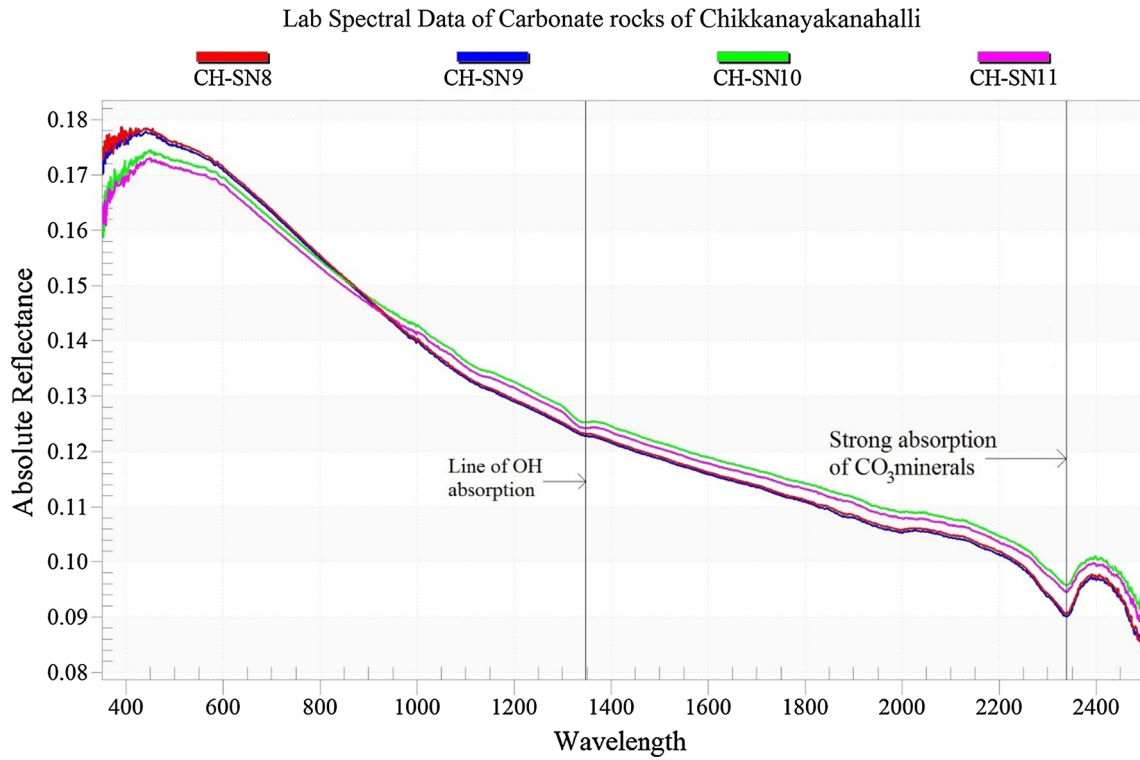
Fig. 3 Spectral plot showing the carbonate mineral absorption (CH-SN8 to CH-SN11 limestone)

Fig. 4 ASTER spectral bands 8, 3, 1 (decorrelated RGB image) of a study area (L1 and L2: limestone deposit)
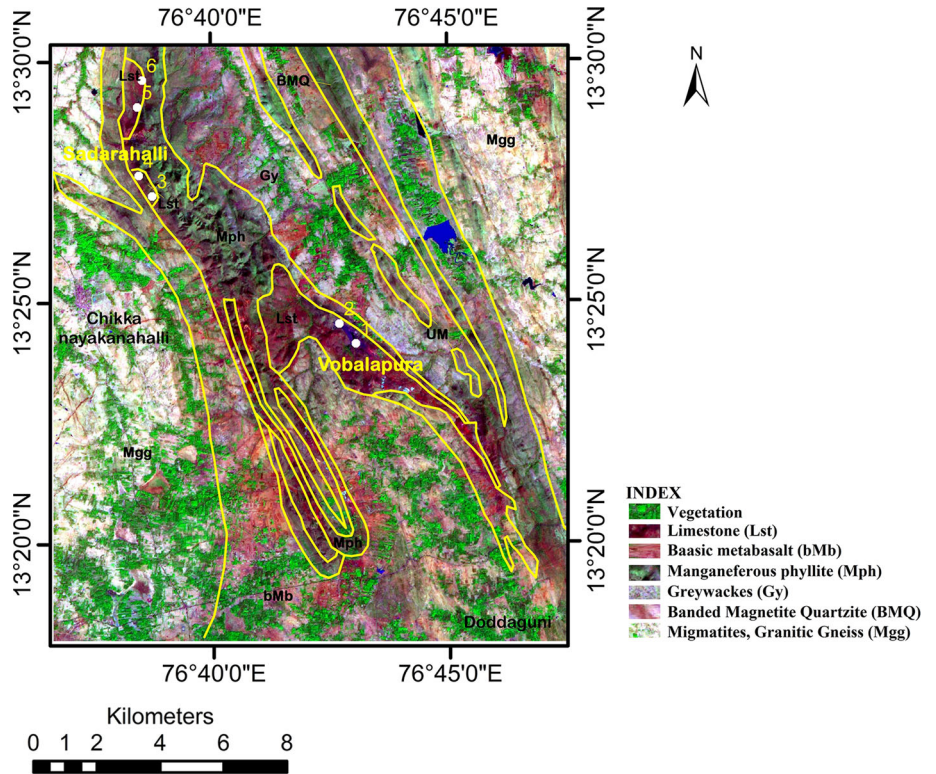
containing 40 percent calcium oxide and 2.80 percent manganese are reported mainly at Vobalapura area. Here, the limestone deposits are being mined for the manufacture of cement by the Mysore Cement Ltd. situated at Ammasandra. There are rich deposits of iron ore and manganese ore all along the schist belt which hosts pockets

Fig. 5 ASTER MNF image (R: B1; G: B2; B: B3) of the study area (Lst: limestone deposit; Mph: manganiferous phyllite; Gy: graywackes; BMQ: banded magnetite quartzite)
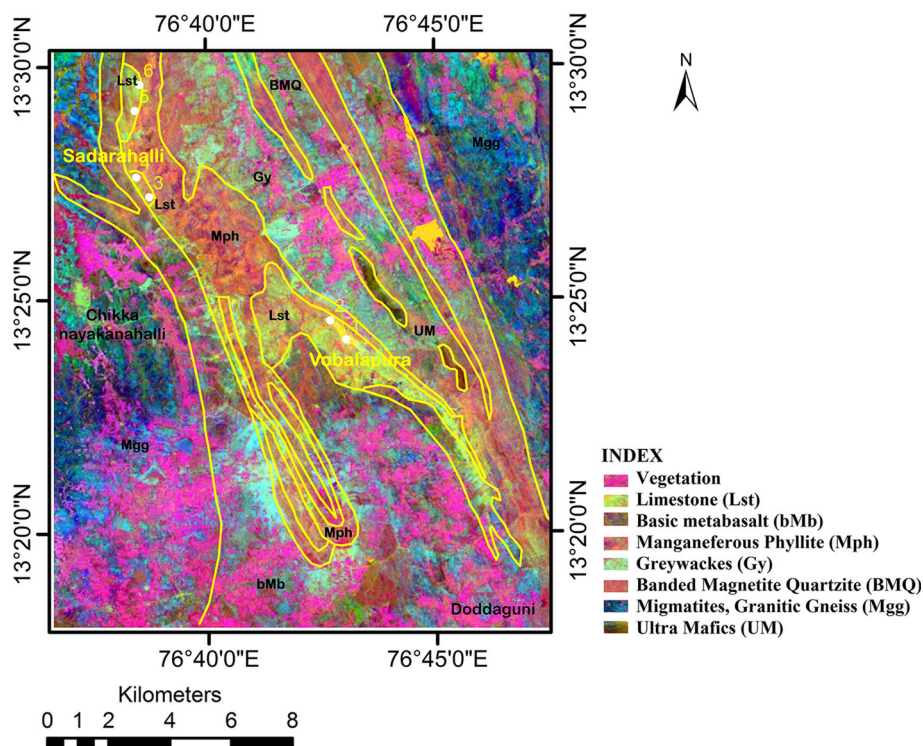
of limestone deposits. These are covered by thin soil cover up to 2 m (Fig. 6a) observed clearly in the mining area. The debris of limestone is found widely in the central part of the study area and toward northwestern part and restricted to pockets of dolo-limestone. These are characterized by the absence of bedding and discontinuity among fragments. Manganese-bearing carbonate formations occurred as isolated and red-colored hills with more or less layering in the area (Fig. 6a–c). In this area, the manganiferous phyllite surrounded by the carbonate formation made the region with structural hills in the schistose zone.

Manganese formation consists of alternate layers of manganese and chert, crystallized into saccharoidal quartz (Garrels 1960; Rowan and Mars 2005), while limestones are observed as pocket within them, and limestones occur in the form of reef-like beds with limited width of outcrop, starting from Doddaguni (SW in the study area) and continuing almost all the western margins of the Chitradurga schist belt. The late Archean banded manganese mineralization in Chikkanayakanahalli region is another important rock types spatially associated with stromatolitic carbonates.

Petrological Characters of Limestone Rock

The minerals and petrographic characters of the limestones of the area are studied by preparation of microscopic thin sections at the Department of Earth Sciences. Under the microscope, the calcite minerals occurred as coarse-grained crystalline texture (Fig. 7a). It shows lamellar twinning in plane polarized light. The deformation twins in the calcite minerals are resulted mainly by relatively low mechanical stress. The sharp contact from one mineral to another mineral shows cryptocrystalline nature of the rock limestone. The study of thin section under the polarized microscope shows that the samples are predominantly occurred with the calcite mineral with the less presence of quartz mineral. The absence of fossil shells and quartz mineral indicates the rocks are chemical sediments. Banded magnetite quartzite is rich with magnetite and appears dark in color due to opaqueness.

Chemical Characters of Carbonate Rocks

To comprehend the spectral reflectance/absorption characters and to validate the image interpretations, the field samples were analyzed for major chemical elements concentrations and the data are given in Table 3. The limestone rocks of Vobalapura area show low content of SiO_2 (18.36–16.38%). These rocks show CaO contents ranged from 38 to 48% and MnO from 1 to 2%. Major chemical elements analysis of selected samples shows the rock with varying CaO composition from 38.70 to 47.61% reveals the presence of calcite in the limestone of the study area. These are responsible to the spectral absorptions of the mineral near 2338 nm (Fig. 3).
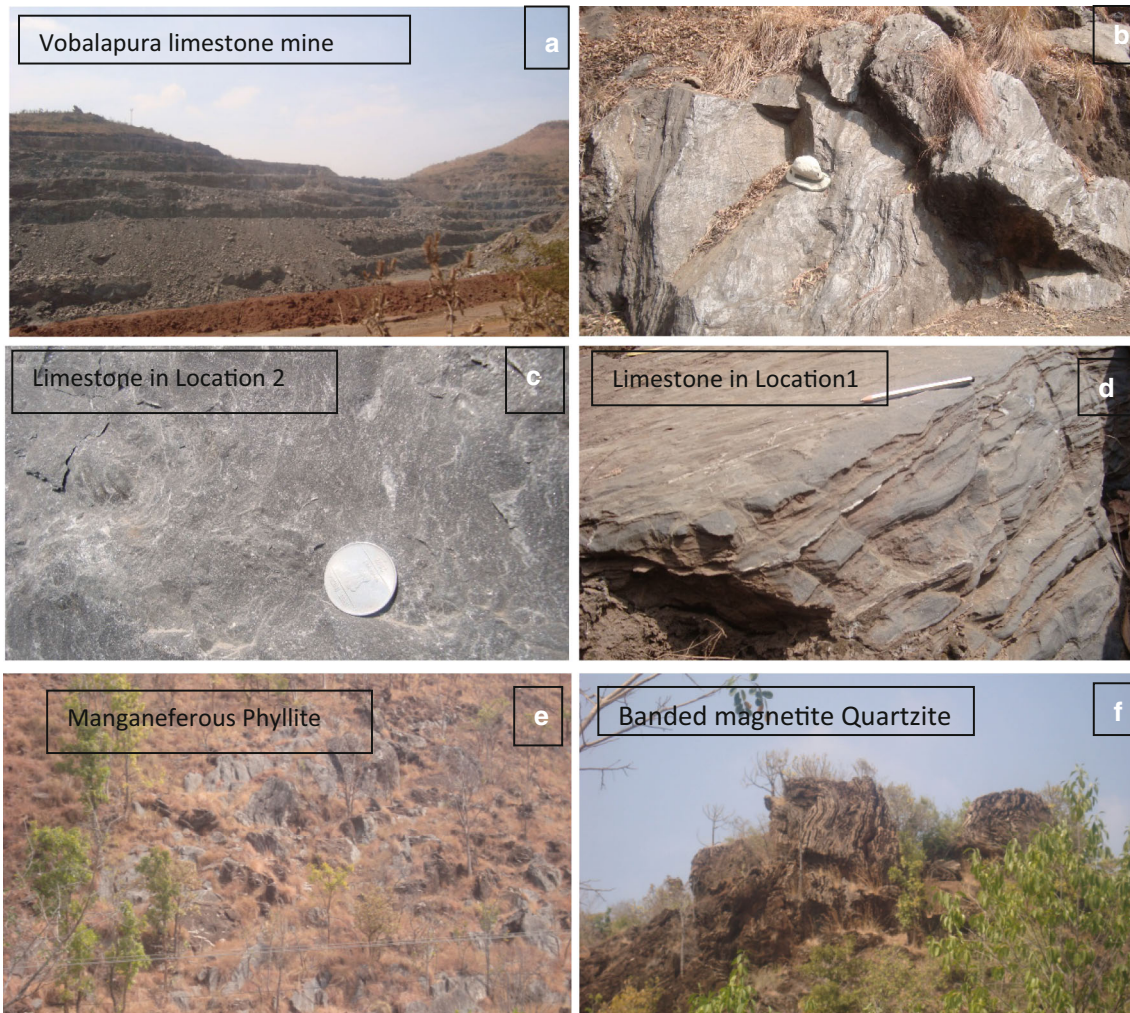
Fig. 6 Field photographs show a. limestone occurences near Guddada Vobalapura village (Location 2), b. dolo-limestone (Location 1), c and d. limestone and dolostone in handspecimen

Results

In this reckful study, the carbonates of Vobalapura (L1) and NW regions (L2) are demarcated visually through the digital image processing methods using ASTER spectral bands 8, 3 and 1 and MNF using the VNIR–SWIR. The CO_3 absorption near 2.35 μm is a clear indication of limestone presence, and based on this spectral sensitivity of carbonate minerals, discriminations are carried out using the ASTER satellite data. The interpretations of limestone formations and associated lithologies of study area are comparable with the available geological map. The limestone formations of Chikkanayakanahalli schist belt are associated with manganiferous phyllite and banded magnetite quartzite, whereas the limestone formations of Proterozoic age is well placed within the Precambrian rocks of the study area. MNF bands assigning to the RGB (R: B1, G: B2, B: B3) showed most of the rock types

clearly in different image tones. Optical studies of samples using petrological microscope confirmed the presence of calcite minerals of the limestone rock. Geochemical analysis rock samples showed varying CaO content from 38.70 to 47.61%, and this result proves the presence of calcite minerals of limestones in the study area. The analyses enlightened the remote sensing application by giving true matched spectra having absorption near 2338 nm. These comprehensive results strengthen the remote sensing application for detailed geological mapping and mineral targeting.

Conclusions

The current study, mapping of limestone deposits and associated rock types of Chikkanayakanahalli region of Chitradurga Schist Belt, Dharwar Craton, is carried out
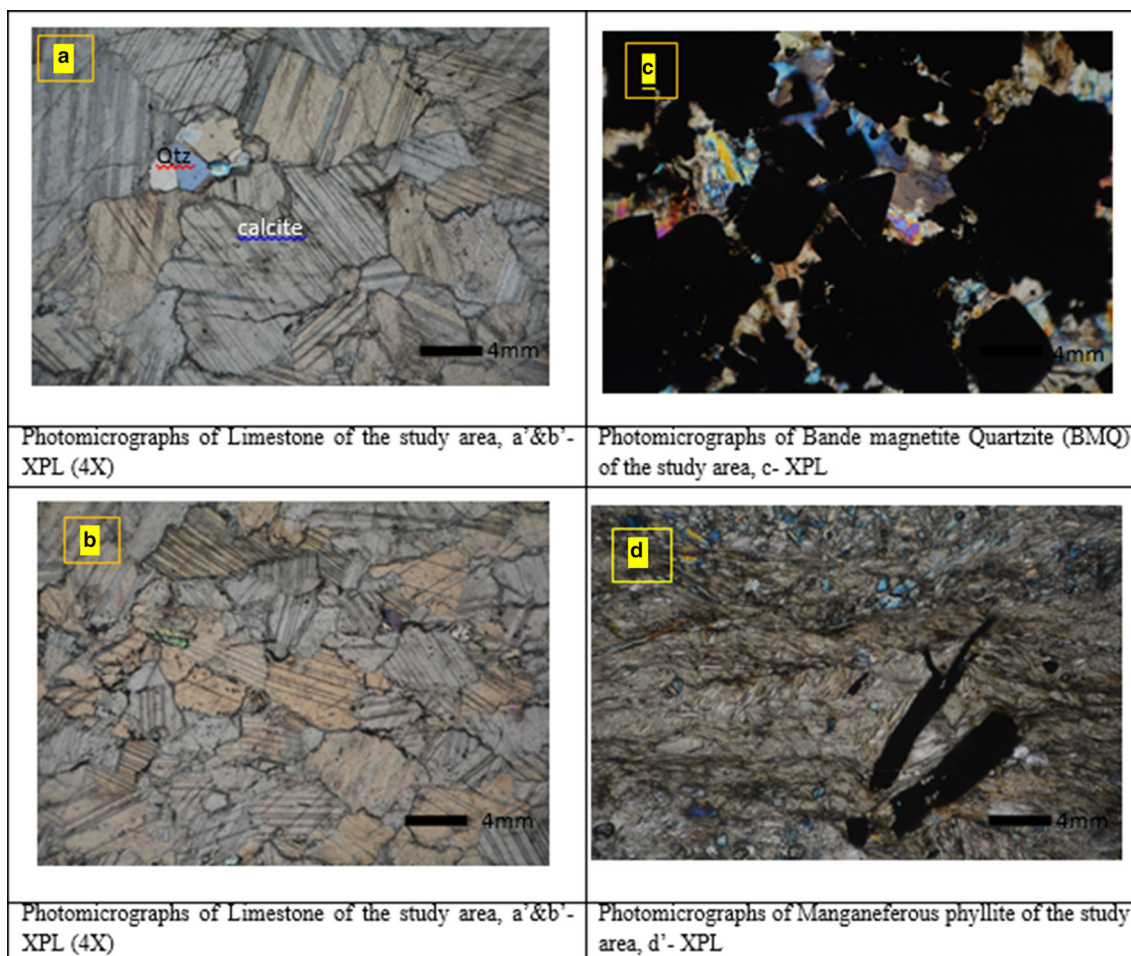
Fig. 7 Photomicrograph shows the carbonate rock mineralogy, i.e., calcite is most essential minerals throughout the rock

Table 3 Major chemical elements of limestones of study area

Laboratory identification (%)	CH-SN8	CH-SN9	CH-SN10	CH-SN11	Upper detection limit	Lower detection limit	Method
SiO2	16.38	16.45	18.17	18.36	100	0.01	IC5870
Al2O3	0.21	0.25	1.96	1.98	100	0.01	IC587
Fe2O3	0.67	0.70	2.24	2.23	100	0.01	IC587
CaO	47.61	48.01	38.98	38.70	100	0.01	IC587
K2O	0.05	0.05	0.62	0.61	10	0.01	IC587
MgO	1.94	1.97	1.67	1.67	100	0.01	IC587
MnO2	0.78	0.82	1.28	1.28	10	0.01	IC587
Na2O	0.05	0.05	0.31	0.31	10	0.01	IC587
TiO2	0.01	0.02	0.06	0.06	10	0.01	IC587
P2O5	0.00	0.00	0.03	0.03	10	0.01	IC587
SO3	0.03	0.02	0.06	0.06	40	0.01	IC587
LOI	42.19	42.26	34.51	34.59	100	0.01	L@950

IC587 4 Acid Digestion ICP OES Finish

LOI@ 950 Loss on Ignition at 950 °C

using ASTER VNIR–SWIR spectral bands. The integration of spectral information with the simple image processing methods delineated the targeted limestone deposits well. In this study, the processing techniques, decorrelation stretching and minimum noise fraction (MNF) methods, showed clearly the distribution of limestone occurrences,

and the results are validated in the field and laboratory studies. The optical studies using petrological microscope and chemical elements analyses showed the presence of calcite minerals in the limestone rock. This study strengthens the remote sensing application for geological mapping of limestone deposits.

References

Abrams, M. (2000). The advanced spaceborne thermal emission and reflection radiometer (ASTER): Data products for the high spatial resolution imager on NASA's Terra platform. *International Journal of Remote Sensing, 21,* 847–859.

Ali, M. Q., Basavarajappa, H. T., & Ranjbar, H. (2009). Application of principal component analysis to ASTER and ETM + data for mapping the alteration zones in North East of Hajjah, Yemen. *Asian Journal of Geoinformatics, 9*(2), 15–21.

Anantha Murthy, K. S. (1980) Carbonates, iron formation, iron and manganese ore deposits of the chiknayakanhalli schist belt Tumkur District, Karnataka. A thesis from Karnataka University.

ASD Inc. (2012). *Field spec specification*. http://www.asdi.com/products/fieldspecspectroradiometers/fieldspec-3-portable-spec troradiometer. Accessed on September 3, 2012.

Baldridge, A. M., Hook, S. J., Grove, C. I., & Rivera, G. (2009). The ASTER spectral library version 2.0. *Remote Sensing Environ, 113,* 711–715.

Bedini, E. (2011). Mineral mapping in the Kap Simpson complex, central East Greenland, using HyMap and ASTER remote sensing data. *Advances in Space Research, 47,* 60–73.

Boardman, J. W., Kruse, F. A., & Green, R. O. (1995). Mapping target signatures via partial unmixing of AVIRIS data. In *Summaries, Proceedings of the 5th JPL Airborne Earth Science Workshop* (95-1, 1: 23–26), January 23–26, Pasadena, California: JPL Publ.

Brandmeier, M. (2010). Remote sensing of Carhuarazo volcanic complex using ASTER imagery in Southern Peru to detect alteration zone and volcanic structures—A combined approach of image processing in ENVI and ArcGIS/ArcScene. *Geocarto International, 25,* 629–648.

Chen, C. M. (2000). Comparison of principal component analysis and Minimum Noise Fraction transformation for reducing the dimensionality of hyperspectral imagery. *Geographical Research, 33,* 163–178.

Clark, R. N. (1999). Spectroscopy of rock and minerals and principles of spectroscopy. In A. N. Rencz (Ed.), *Remote sensing for the earth sciences: Manual of remote sensing* (3rd ed., Vol. 3, pp. 3–58). New York: Wiley.

Clark, R. N., Swayze, G. A., Heidebrecht, K., Green, R. O., & Goetz, A. F. H. (1995) Calibration to surface reflectance of terrestrial imaging spectrometry data: Comparison of methods. In *Summaries of the 5th Annual JPL Airborne Geosciences Workshop* (pp. 41–42). Jet Propulsion Laboratory Special Publication.

Crosta, A. P., Filho, C. R. D. S., Azevedo, F., & Brodie, C. (2003). Targeting key alteration minerals in epithermal deposits in Patagonia, Argentina, using ASTER imagery and principal component analysis. *International Journal of Remote Sensing, 24,* 4233–4240.

Crowley, J. K. (1986). Visible and near-infrared spectra of carbonate rocks: Reflectance variations related to petrographic texture and impurities. *Journal Geophysical Research, 91,* 5001–5012.

Devaraju,T. C., & Anathmurthy, K. S. (1977) Iron and manganese ores of C.N. halli schist belt, Tumkur district. In C. Naganna & B. Somashekar (Eds.) *Proceedings of the first symposium on the geology, exploration, mining processing and metallurgy of ferrous and ferro-alloy minerals* (pp. 22–31).

Devaraju, T. C., & Anathmurthy, K. S. (1984). Carbonates of Chikkanayakanahalli schist belt, Karnataka. *The Journal of the Geological Society of India, 25,* 162–174.

ENVI. (2009). *Atmospheric Correction Module: QUAC and FLAASH User's Guide*. http://www.exelisvis.com/portals/0/pdfs/envi/Flaash_Module.pdf2009.

Gaffey, S. J. (1985). Reflectance spectroscopy in the visible and near infrared (0.35–2.55 microns): Applications in carbonate petrology. *Geology, 13,* 270–273.

Gaffey, S. J. (1986a). Spectral reflectance of carbonate minerals in the visible and near infrared (0.35–2.55 microns): Calcite, aragonite, and dolomite. *American Mineralogist, 71,* 151–162.

Gaffey, S. J. (1986b). Spectral reflectance of carbonate minerals in the visible and near infrared (0.35–2.55 microns): Calcite, aragonite, and dolomite. *American Mineralogist, 71,* 151–162.

Gaffey, S. J. (1987). Spectral reflectance of carbonate minerals in the visible and near infrared (0.35–2.55 microns): Anhydrous carbonate minerals. *Journal Geophysical Research, 92*(B2), 1429–1440.

Garrels, R. M. (1960). *Mineral Equilibria* (p. 254). Newyork: Harper and brothers.

Ghosh, S. K., & Chatterjee, B. K. (1990). Paleoenvironment reconstruction of early Proterozoic Kolhan siliciclastic rocks, Keonjhar districts, Orissa, India. *Journal Geological Society of India, 35,* 273–286.

Green, A. A., Berman, M., Switzer, P., & Craig, M. D. (1988). A transformation for ordering multispectral data in terms of image quality with implications for noise removal. *IEEE Transactions on Geoscience Remote Sensing, 26*(1), 65–74.

Guha, A., Rao, A., Ravi, S., Vinod Kumar, K., & Dhananjaya Rao, E. N. (2012a). Analysis of the potential of kimberlite rock spectra as spectral end member using samples from Narayanpet kimberlite Field (NKF), Andhra Pradesh. *Current Science, 103*(9), 1096–1104.

Guha, A., et al. (2012b). Spectroscopic study of rocks of Hutti-Maski Schist Belt, Karnataka. *Journal Geological Society of India, 79,* 335–344.

Gupta, R. P. (2003). *Remote Sensing Geology* (2nd ed.). Heidelberg: Springer.

Hamilton, W. R., Wolley, A. R., & Bishop, A. C. (1995). *Hamlyn guide: Minerals, rocks and fossils*. Hong Kong: Mandarin Offset.

Harding, D. J., Wirth, K. R., & Bird, J. M. (1989). Spectral mapping of Alaskan ophiolites using landsat thematic mapper data. *Remote Sensing of Environment, 28,* 219–232.

Haselwimmer, C. E., Riley, T. R., & Liu, J. G. (2011). Lithologic mapping in the Oscar II Coast area, Graham Land, Antarctic Peninsula using ASTER data. *International Journal of Remote Sensing, 32*(7), 2013–2035. https://doi.org/10.1080/01431161003645824.

Hubbard, B. E., & Crowley, J. K. (2005). Mineral mapping on the Chilean– Bolivian Altiplano using co-orbital ALI, ASTER and Hyperion imagery: Data dimensionality issues and solutions. *Remote Sensing Environment, 99,* 173–186.

Hunt, G. R., & Salisbury, J. W. (1970). Visible and near-infrared spectra of minerals and rocks. *Modern Geology, 1*, 283–300.

Jensen, J. R. (2005). *Introductory digital image processing*. Upper Saddle River: Person Prentice Hall.

Kalinowski, A., & Oliver, S. (2004). *ASTER mineral index processing manual*. http://www.ga.gov.au/image_cache/GA7833.pdf.

Khan, S. D., Mahmood, K., & Casey, J. F. (2007). Mapping of Muslim Bagh ophiolite complex (Pakistan) using new remote sensing, and field data. *Journal of Asian Earth Science, 30*, 333–343.

Mars, J. C., & Rowan, L. C. (2010). Spectral assessment of new ASTER SWIR surface reflectance data products for spectroscopic mapping of rocks and minerals. *Remote Sensing Environment, 114*, 2011–2025.

Mukhopadhyay, D., Baral, M. C., & Ghosh, D. (1981). A tectonostratigraphic model of the Chitradurga schist belt, Karnataka, India. *Journal of the Geological Society of India, 22*, 22–31.

Mukhopadhyay, D., & Ghosh, D. (1983). Superposed deformation in the Dharwar rocks of the Southern part of the Chitradurga schist belt near Dodguni, Karnataka. *Geological Science India Memoir, 4*, 275–292.

Mukhopadhyay, J., Ghosh, G., Nandi, Ajoy K., & Chaudhuri, A. K. (2006). Depositional setting of the Kolhan Group: Its implications for the development of a Meso to Neoproterozoic deep-water basin on the South Indian Craton. *South African Journal of Geology, 109*, 183–192.

Philip, G., Ravindran, K. V., & Mathew, J. (2003). Mapping the Nidar ophiolite complex of the Indus suture zone, Northwestern-Trans Himalaya using IRS-1C/1D data. *International Journal of Remote Sensing, 24*, 4979–4994.

Pour, A. B., & Hashim, M. (2011a). Spectral transformation of ASTER data and the discrimination of hydrothermal alteration minerals in a semi-arid region, SE Iran. *International Journal of the Physical Sciences, 6*(8), 2037–2059.

Pour, B. A., & Hashim, M. (2011b). Application of advanced spaceborne thermal emission and reflection radiometer (ASTER) data in geological mapping. *International Journal of Physical Sciences, 6*, 7657–7668.

Pournamdari, M., Hashim, M., & Pour, A. B. (2014a). Spectral transformation of ASTER and Landsat TM bands for lithological mapping of Soghan ophiolite complex, South Iran. *Advances in Space Research, 54*, 694–709.

Pournamdari, M., Hashim, M., & Pour, A. B. (2014b). Application of ASTER and Landsat TM data for geological mapping of Esfandagheh ophiolite complex, southern Iran. *Resource Geology, 64*, 233–246.

Radhakrishna, B. P. (1952). Proceedings of the Indian Science Congress 39th Session, IV (p 181).

Rajendran, S., Al-Khirbash, S., Pracejus, B., Nasir, S., Al-Abri, A. H., Kusky, T. M., & Ghulam, A. (2012). ASTER detection of chromite bearing mineralized zones in Semail Ophiolite Massifs of the northern Oman Mountain: Exploration strategy. *Ore Geology Reviews, 44*, 121–135.

Rajendran, S., Hersi, O. S., Al-Harthy, A., et al. (2011). Capability of advanced spaceborne thermal emission and reflection radiometer (ASTER) on discrimination of carbonates and associated rocks and mineral identification of eastern mountain region (Saih Hatat window) of Sultanate of Oman. *Carbonates and Evaporites, 26*, 351. https://doi.org/10.1007/s13146-011-0071-4.

Rajendran, S., & Nasir, S. (2013). ASTER spectral analysis of ultramafic lamprophyres (carbonatites and aillikites) within the Batain nappe, northeastern margin of Oman: A proposal developed for spectral absorption. *International Journal of Remote Sensing, 34*(8), 2763–2795.

Rajendran, S., & Nasir, S. (2014a). Hydrothermal altered serpentinized zone and a study of Ni-magnesioferrite-magnetite-awaruite occurrences in Wadi Hibi, Northern Oman Mountain: Discrimination through ASTER mapping. *Ore Geology Reviews, 62*, 211–226.

Rajendran, S., & Nasir, Sobhi. (2014b). ASTER mapping of limestone formations and study of caves, springs and depressions in parts of Sultanate of Oman. *Environmental Earth Sciences, 71*, 133–146.

Rajendran, S., & Nasir, Sobhi. (2014c). ASTER spectral sensitivity of carbonate rocks: Study in Sultanate of Oman. *Advances in Space Research, 53*, 656–673.

Ramakrishna, B. P., & Vaidyanadhan, R. (2008). *Geology of Karnataka*. India: Geol Soc.

Rowan, L. C., & Mars, J. C. (2003). Lithologic mapping in the Mountain Pass, California area using Advanced Speceborne Thermal Emission and Reflection Radiometer (ASTER) data. *Remote Sensing of Environment, 84*, 350–366.

Rowan, L. C., & Mars, J. C. (2005). Lithologic mapping of the Mordor, NT, Australia ultramafic complex by using the Advanced Spaceborne Thermal Emission and Reflection Radiometer (ASTER). *Remote Sensing of Environment, 99*, 105–126.

Sanjeevi, S. (2008). Targeting limestone and bauxite deposits in southern India by spectral unmixing of hyperspectral image data. In *The international archives of the photogrammetry, remote sensing and spatial information sciences ISPRS congress Beijing*, Vol. XXXVII, Part B8, Commission VIII, Beijing, p. 1189.

Srinivasan, R., Shukla, M., Naqvi, S. M., Yadav, V. K., Venkatachala, B. S., Uday Raj, B., et al. (1989). Archaean stromatolites from the Chitradurga schist belt, Dharwar craton, South India. *Precambrian Research, 43*, 239–250.

Srinivasan, R., & Srinivas, B. L. (1972). Dharwar stratigraphy. *Journal of the Geological Society of India, 13*, 72–83.

Swaminath, J., Ramakrishnan, M., & Viswanatha, M. N. (1976). Dharwar stratigraphic model and Karnataka craton evolution. *Records of the Geological Survey of India, 107*(2), 149–175.

Van der Meer, F. (1994). Extraction of mineral absorption features from high spectral resolution data using non parametric geostatistical techniques. *International Journal of Remote Sensing, 15*(11), 2193–2214.

Van der Meer, F. (1995). Spectral reflectance of carbonate mineral mixtures and bidirectional reflectance theory: Quantitative analysis techniques for application in remote sensing. *Remote Sensing Reviews, 13*, 67–94.

Yamaguchi, Y. I., Fujisada, H., Kudoh, M., Kawakami, T., Tsu, H., Kahle, A. B., et al. (1999). ASTER instrument characterization and operation scenario. *Advances in Space Research, 23*(8), 1415–1424.

Zhang, X., Pazner, M., & Duke, N. (2007). Lithologic and mineral information extraction for gold exploration using ASTER data in the south Chocolate Mountains (California). *ISPRS Journal of Photogrammetry and Remote Sensing, 62*, 271–282.